Available online at www.sciencedirect.com
SCIENCE DIRECT®
Journal of Power Sources 119–121 (2003) 631–636
JOURNAL OF POWER SOURCES
www.elsevier.com/locate/jpowsour

Lithium-7 nuclear magnetic resonance and Ti K-edge X-ray absorption spectroscopic investigation of electrochemical lithium insertion in $Li_{4/3+x}Ti_{5/3}O_4$

Fabio Ronci[a], P.E. Stallworth[b], Faisal Alamgir[b], Theanne Schiros[b], Jason Van Sluytman[b], Xiaodong Guo[b], Priscilla Reale[a], Steve Greenbaum[b,*], Marten denBoer[b], Bruno Scrosati[a]

[a]*Department of Chemistry, University of Rome, La Sapienza, Rome 00185, Italy*
[b]*Department of Physics, Hunter College of CUNY, 695 Park Avenue, NY 10021, USA*

Abstract

The spinel compound $Li_{4/3+x}Ti_{5/3}O_4$ is known to undergo reversible lithium intercalation up to $x = 1$ with almost no change in lattice parameters, hence its designation as a "zero strain" intercalation compound. Structural changes that accompany electrochemical Li intercalation into this compound were studied by both ^{7}Li nuclear magnetic resonance (NMR) and Ti K-edge X-ray absorption fine structure (XAFS). The NMR results demonstrate that Li occupancies do not follow a simple distribution between two possible sites, one tetrahedral and one octahedral. The presence of at least one additional octahedral site is suggested. Line width measurements show that the Li^+ ions do not return to their original distribution after cycling. XAFS results indicate the presence of modest static disorder in Ti–O and Ti–Ti distances above $x = 0.5$. Both methods thus reveal subtle structural details previously unobserved by X-ray diffraction (XRD).

Keywords: ^{7}Li nuclear magnetic resonance; Ti K-edge X-ray absorption fine structure; $Li_{4/3+x}Ti_{5/3}O_4$

1. Introduction

The spinel lithium titanate $Li_{4/3}Ti_{5/3}O_4$ is a well known electrode material for Li-ion batteries, capable of reversibly intercalating lithium ions up to $Li_{7/3}Ti_{5/3}O_4$, i.e. $0 < x < 1$ in $Li_{4/3+x}Ti_{5/3}O_4$ [1,2]. The parent compound denoted by $x = 0$ is a member of the $Li_{1+y}Ti_{2-y}O_4$ family ($0 < y < 1/3$). These latter compositions have been studied for superconductivity properties, including $LiTi_2O_4$, the first discovered superconductor having $T_C > 10$ K [3]. $Li_{4/3}Ti_{5/3}O_4$ has a spinel crystallographic structure, space group $Fd3m$, and is better described, using the Wyckoff formalism, as $[Li]_{8a}[Li_{1/3}Ti_{5/3}]_{16d}[0_4]_{32e}$. The attractive electrochemical characteristics of $Li_{4/3+x}Ti_{5/3}O_4$ are its flat discharge curve and its negligible structural variations upon cycling (zero strain insertion). This intercalation compound has been extensively studied from the electrochemical point of view, but only recently it has been possible to study the very subtle structural changes that occur upon intercalation. By using both ex situ [4,5] and, more recently, in situ X-ray diffraction (XRD) studies [6,7], the intercalation process has been described as a two-phase equilibrium between a lithium-poor ($Li_{4/3+x}Ti_{5/3}O_4$, with $x \sim 0.03$–0.17) and a lithium-rich phase ($Li_{7/3}Ti_{5/3}O_4$). The most peculiar evidence is that these two cubic structures, differing only in the lithium ion sublattice, show almost identical lattice parameters, with a difference of about 0.07% [5,7]. It has also been pointed out that upon insertion the excess lithium becomes distributed about tetrahedral 8a and newly created octahedral 16c sites, such that when the maximum amount of inserted lithium is attained ($x = 1$) 8a sites are converted to 16c sites, i.e. $[Li_2]_{16c}[Li_{1/3}Ti_{5/3}]_{16d}[0_4]_{32e}$ [4]. Still, within the limiting compositions ($x = 0$ and 1), details regarding the distribution of lithium sites are not complete.

The utilization of other techniques could be useful towards a deeper understanding of the intercalation process of this compound. Several nuclear magnetic resonance (NMR ^{7}Li, ^{6}Li, ^{47}Ti and ^{49}Ti) studies have been reported for $Li_{1+y}Ti_{2-y}O_4$ [8–10] and X-ray absorption fine structure (XAFS) measurements have been performed on different titanium oxides [11,12]. However, to the best of our knowledge, neither NMR or XAFS studies have been reported for $Li_{4/3+x}Ti_{5/3}O_4$, where $x > 0$. X-ray techniques are not well suited to probe lithium environments; however, ^{7}Li NMR is quite sensitive, and therefore is a particularly important

* Corresponding author.
E-mail address: steve.greenbaum@hunter.cuny.edu (S. Greenbaum).

0378-7753/03/$ – see front matter
doi:10.1016/S0378-7753(03)00191-5

measurement. In this paper, we report on static ^{7}Li NMR and XAFS Ti-edge studies of deintercalated $Li_{4/3+x}Ti_{5/3}O_4$ samples. The information gathered from these measurements is pertinent to the lithium site distribution and titanium reduction upon lithium insertion.

2. Experimental

2.1. Sample preparation

$Li_{4/3}Ti_{5/3}O_4$ for NMR measurements was synthesized by a solid-state route, thoroughly mixing $LiOH{\cdot}H_2O$ and TiO_2 and then annealing at 800 °C for 16 h. The compound was ground together with 8% conductive carbon, "Super P" (Super P:titanate = 8:92), and pellets of about 100 mg were prepared using a pressure of approximately 5 t/cm^2. Smaller quantities of material (less than half) were used in a somewhat thinner configuration for the XAFS samples. The pellets were inserted in lithium cells using $LiClO_4$ EC:DMC electrolyte. A discharge current of $C/100$ (1 equivalent of inserted lithium in 100 h) was imposed in order to ensure uniform intercalation for the thicker samples, and the following intercalation states were reached for $Li_{4/3+x}Ti_{5/3}O_4$: $x = 0$ ($Li_{4/3}Ti_{5/3}O_4$ + Super P as prepared), $x = 0.75$, 1.00, and $x = 0$ (after one whole cycle). The cells were opened inside a dry-box and the pellets for NMR investigation were carefully washed with acetonitrile to remove any residual electrolyte salt.

2.2. NMR measurements

Variable temperature ^{7}Li ($I = 3/2$) NMR measurements were performed on a Chemagnetics CMX 300 spectrometer operating at 116.99 MHz (field strength of 7.1 T) where a saturated aqueous solution of LiCl was used as the ^{7}Li reference. The spectra were gathered using both phase cycled *pulse*–delay–acquire (one-pulse) and *pulse*–τ–*pulse*–τ–acquire (quadrupolar echo, 25 μs < τ < 50 μs) sequences followed by Fourier transformation (FT) of the free-induction decay or the trailing half-echo. At room temperature, excitation pulse lengths of 2.0 μs gave maximum signal strengths and dead time delays of 10 μs or more were employed. Measurements were performed at −150 and 23 °C and were carried out by channeling dry N_2 gas, at the desired temperature, through the NMR probe to the sample. Slight broadening of the line occurred at lower temperatures and the corresponding excitation pulse length reduced to about 1.6 μs.

Room temperature spin-lattice relaxation times (T_1), as determined by inversion and saturation methods, were approximately 9 s for all compositions; and in this regard for normal acquisition of the free-induction decay, delays of about 60 and 120 s (at 295 and 123 K, respectively) were used after each transient. It is noted that Dalton et al. [8] find $T_1 = 71$ s for the parent compound, $Li_{4/3}Ti_{5/3}O_4$ which was prepared by solid-state reaction of the starting materials. The variation in T_1 between this and the present work is attributed to structural differences manifested between the materials prepared by solid-state reaction using Li_2CO_3 and those using LiOH. As stated above, Super P conductive carbon has been incorporated into the present electrochemically prepared samples and the degree to which this might affect the ^{7}Li relaxation is assumed to be negligible.

2.3. X-ray absorption measurements

X-ray absorption spectra were acquired in transmission mode at the X23A2 beamline of the National Synchrotron Light Source located at the Brookhaven National Laboratory. The monochromator crystal used was a Si(3 1 1). The signals were collected in transmission using N_2-filled ion chamber detectors. The details of standard data transformation from absorption to a function that is proportional to the radial distribution function are given elsewhere [13].

3. Results: NMR

As demonstrated by Dalton et al. [8] for $Li_{4/3}Ti_{5/3}O_4$, ^{7}Li lines are broadened by homonuclear dipolar interactions and to a lesser extent chemical shift interactions. This combined effect does not yield resolved spectra for the distinct lithium sites at natural abundance even with magic angle spinning (MAS). However, ^{6}Li enrichment allows for the observation of some features within the central transition, and these have been assigned to lithium ions in the spinel octahedral and tetrahedral sites (here designated as 16d and 8a, respectively) [4]. These results have been further substantiated by ^{6}Li NMR [10].

Previous electrochemical and X-ray diffraction characterizations suggest that the following reaction takes place upon insertion [4,5]:

$$[Li]_{8a}[Li_{1/3}Ti_{5/3}]_{16d}[O_4]_{32e} + xe^- + xLi^+ \Leftrightarrow [Li_{1+x}]_{8a,16c}[Li_{1/3}Ti_{5/3}]_{16d}[O_4]_{32e} \quad \text{for } 0 < x \leq 1, \tag{1}$$

where at $x = 1$, 8a sites are assumed to be entirely converted into 16c sites. As mentioned earlier, interpretations have been based on two coexisting interconvertible phases, $Li_{4/3}Ti_{5/3}O_4$ and $Li_{7/3}Ti_{5/3}O_4$.

In the present work, ^{7}Li static wide-line spectra are superpositions of lithium lines due to various environments. Representative spectra are displayed in Fig. 1. NMR spectra obtained at room temperature show slight motional narrowing, therefore in order to get a better representation of the satellites, the spectra in Fig. 1 were gathered at −150 °C. A large central line is generally observed and upon lithium insertion weaker features indicative of first-order quadrupolar broadened satellites can be found. Such features are observed for small tetragonal distortions and cylindrically symmetric environments about lithium atoms, and

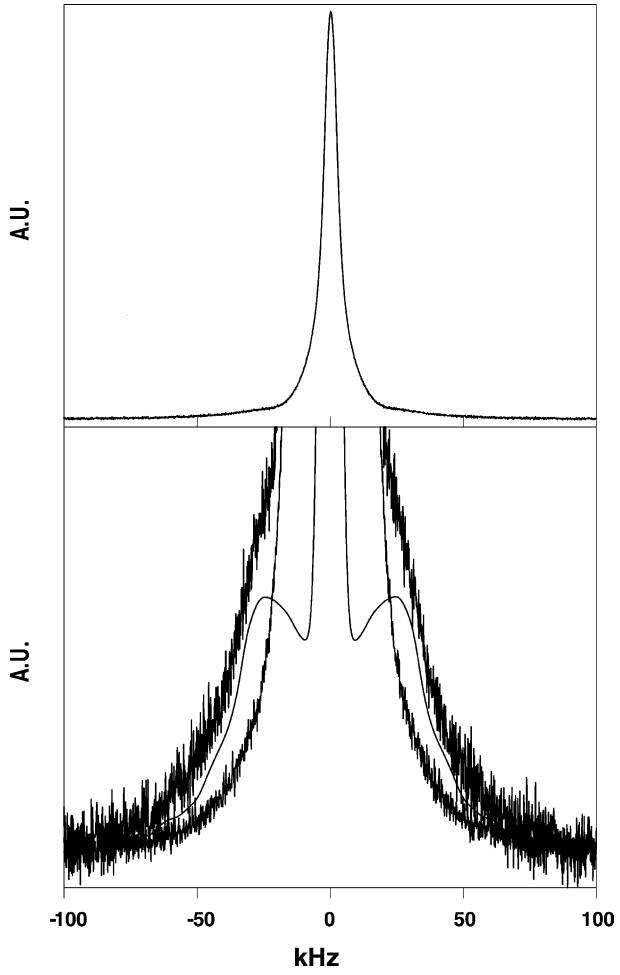

Fig. 1. ^{7}Li NMR spectra of $Li_{4/3+x}Ti_{5/3}O_4$: outer spectrum, $x = 1$; inner spectrum, $x = 0$; smooth curve in between spectra, simulated resonance with quadrupole parameters cited in text. Chemical shift range is too small to differentiate octahedral and tetrahedral lithium sites at natural abundance. Increased intensity of quadrupolar broadened satellites is correlated with larger lithium contents.

are verified to be quadrupolar because their intensity is enhanced relative to the central transition in the quadrupolar echo data. The satellites become more prominent with insertion and the analysis of these features provides some insight into the lithium distribution with x.

The satellites are not observed at $x = 0$, and in this respect are not associated with the tetrahedral 8a lithium site. This composition has been previously studied by NMR, and an interpretation based on 8a and 16d sites has been made according to the intercalation reaction (1) shown above [8]. Considering the possible remaining sites (i.e. for $x = 0$, the lithium ions are distributed over tetrahedral 8a and newly created octahedral 16c sites), it is then suggested that the increased satellite intensity (for $x = 0.75$ and 1.00) is associated with the increased occupation of the 16c octahedral site. Line component intensities in pulsed NMR spectra are subject to pulse response differences between the central and satellite transitions and finite pulse-width distortions [14]. Nevertheless, the former can be analyzed through simulation and the latter minimized through the use of small pulse widths, as was done for these measurements. Analysis demonstrates that approximately 20% or less of the total line intensity for the $x = 1$ material can be assigned to the site(s) exhibiting the satellite features. However, this estimate is far lower than expected for the 16c site occupation as given by references [4,5]. Simulations of the satellites yield the average values: $e^2qQ/h = Q_{cc} \sim 130$ kHz and $\eta = 0$. The observed quadrupolar features are associated with a site that becomes more populated, along with the 16c sites, with increasing lithium content; and therefore, indicate that lithium 8a tetrahedral sites are not simply converted to 16c octahedral sites on insertion, according to the intercalation reaction (1). The unambiguous identification of the site responsible for the quadrupolar features remains as the primary task for further study. It is reasonable to speculate on a number of Frenkel and Schottky defect states. These have been considered by Ammundsen et al. in their simulation study of Mn_2O_4–λMnO_2 spinels [15].

Further insight into the insertion process can be obtained from the line width data given in Fig. 2. These data generally reflect the magnetic interactions that ^{7}Li nuclei encounter as a function of lithium content. The parent compound is diamagnetic, whereby upon lithium insertion, more Ti^{4+} is reduced to Ti^{3+} and the compound becomes paramagnetic. The line width increase with lithium content is consistent with increased homonuclear dipolar (^{7}Li–^{7}Li) and paramagnetic interactions (^{7}Li–Ti^{3+}). Interestingly, significantly larger ^{7}Li line widths are obtained for the cycled sample ($x = 0$). This suggests that at least over the first cycle, the distribution of Li sites becomes less

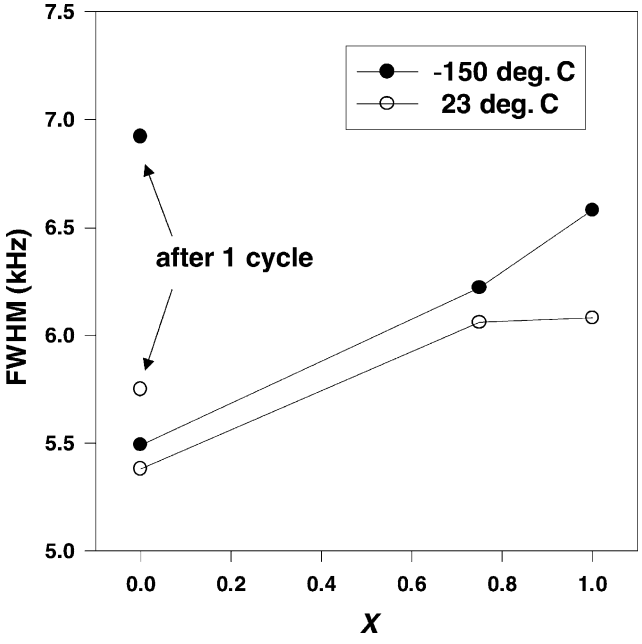

Fig. 2. ^{7}Li NMR central transition line widths vs. Li content reveal slight motional narrowing at room temperature. Irreversible characteristics are apparent in that line widths increase significantly after one cycle.

random (e.g. depopulation of surface states and clustering of interior 16d sites) and on average the proximity between lithium sites decreases.

4. X-ray absorption

It is observed from the X-ray absorption near-edge structure (XANES) that the conduction band of the $Li_{4/3+x}Ti_{5/3}O_4$ cathode undergoes a discontinuous change during the discharge of the cell as x increases from 0 to 1 (Fig. 3). The maxima in the first two peaks in the XANES is clearly delineated into two different groups, viz. the region at and before $x = 0.5$ and the region at and after $x = 0.75$. There is no change in the conduction band density of states (DOS) until at least 50% of the total amount of Li has intercalated into the cathode, and this change is already saturated by the time the 75% of the Li has entered the cathode. The DOS for the cathode which had been cycled multiple times appears to be similar to that of the fully discharged cell.

In the EXAFS portion of the spectrum, ~50 eV above the absorption edge, the photoelectron is not as sensitive to the

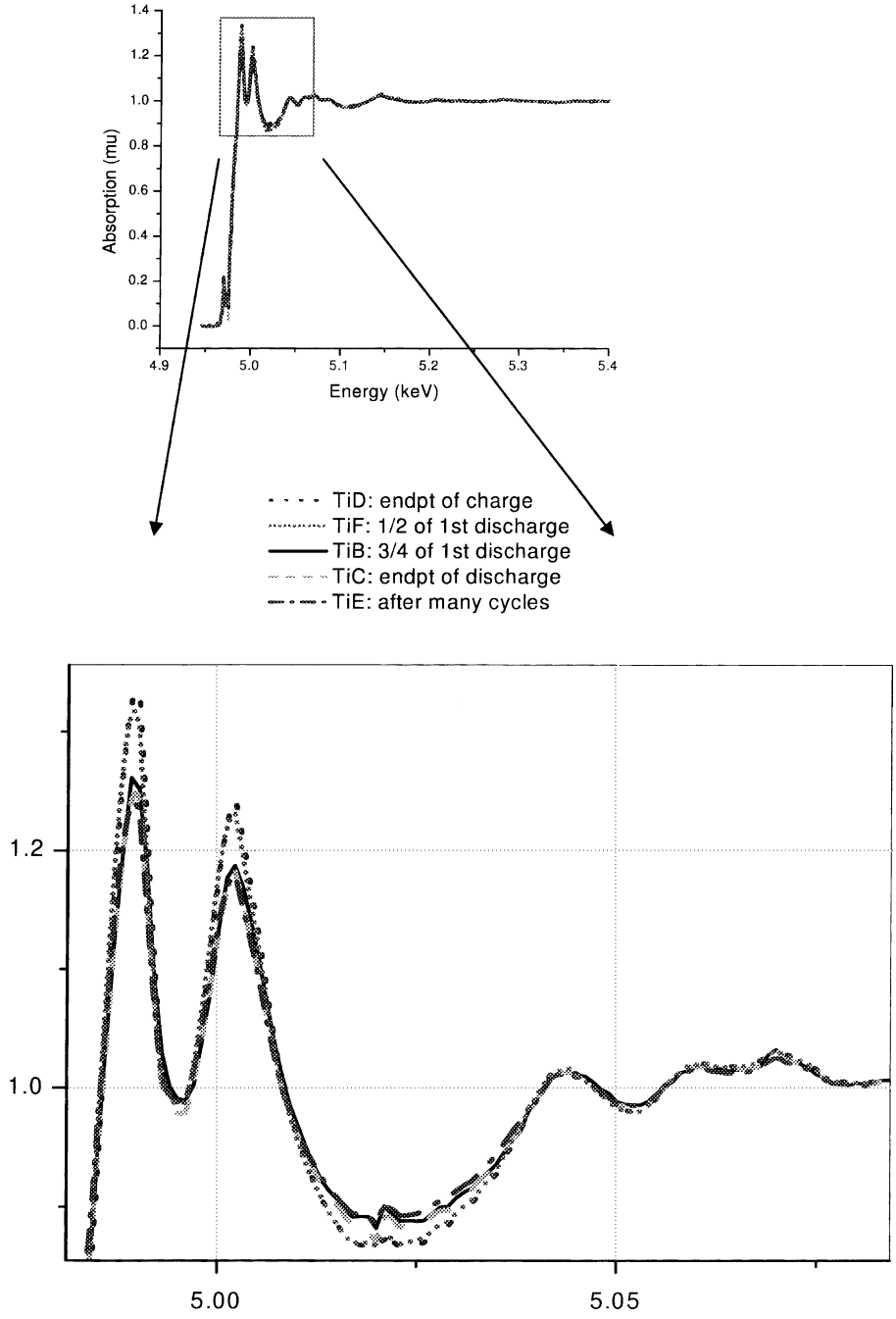

Fig. 3. Ti K-edge absorption spectrum vs. energy for the cathode at different levels of cell discharge. Horizontal scale is in units of keV.

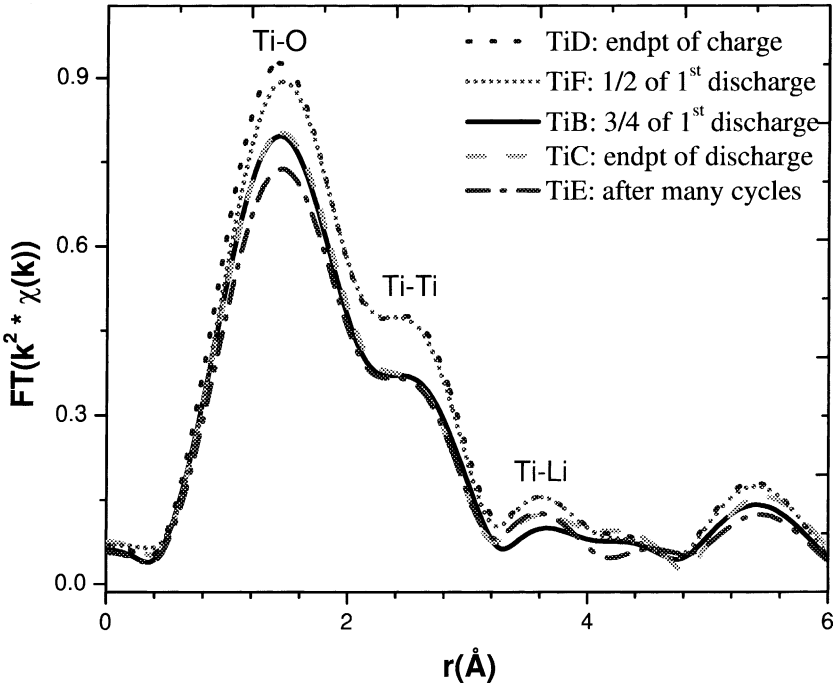

Fig. 4. Fourier transforms of the weighted $[k^2\chi(k)]$ EXAFS functions (closely related to the radial distribution function) for a series of titanate cathodes ($Li_{4/3+x}Ti_{5/3}O_4$) obtained at various stages of the charge/discharge.

local electronic structure and more sensitive to the distribution of atomic potentials. The isolation of this fine structure in k-space ($\chi(k)$) and its subsequent k^2-weighted Fourier transform to real space yields a function proportional to the radial distribution function. In Fig. 4 is plotted the FT $[(k^2\chi(k))]$ for the samples as a function of Li content. An inspection of the positions of the Ti–O and Ti–Ti neighbors reveals that they don not change upon Li intercalation (discharge). This is consistent with the previously mentioned XRD findings that show insignificant change in lattice parameter over the full range of Li insertion [5,7]. It is further observed that during the discharge, the total scattering amplitude is reduced as a function of increased lithium content in the cathode during the discharge cycle. Within the single discharge process, the amplitudes of FT $[k^2\chi(k)]$ at the Ti–Ti distance do not undergo any change until at least $x = 0.5$, or halfway through the discharge path. This is followed by a significant reduction in the amplitude in the range $0.5 < x < 0.75$. By $x = 0.75$, this change has saturated. Amplitude reduction at the Ti–O bond distance in the range $0.5 < x < 0.75$ and above is also observed. These subtle effects exposed by EXAFS have not been observed by earlier work using X-ray diffraction [5]. Scharner et al. observe a continuous change in the (0 4 8), (4 4 8) and the (1 5 9) reflections as a function of Li intercalation that begins before $x = 0.5$, and ends after $x = 0.75$. EXAFS reveals that the changes observed by Scharner et al. do not involve Ti atoms below $x = 0.5$ and after $x = 0.75$. That is, while these authors suggest a two-phase reaction from their observed changes in XRD reflections, their interpretations may be limited by a lack of local structural information. With such information available from EXAFS, at least one intermediate step needs to be included in the reaction. Lithium insertion proceeds first without the disruption of Ti–Ti coordination, followed by at least one reaction in the $0.5 < x < 0.75$ range where the Ti–Ti peak begins to be affected, and perhaps a second modest structural rearrangement in the $0.75 < x < 1.0$ range. The full width at half maximum of the Ti–Ti RDF peak is somewhat larger than for $x = 0.75$. The amplitude reduction for both the Ti–O and the Ti–Ti bonds can be simulated by increasing the static disorder at both these distances. Finally, multiple cycling appears to produce a similar increase in static disorder, for both Ti–O and Ti–Ti distances.

5. Discussion and conclusions

This report presents complementary structural information on the $Li_{4/3+x}Ti_{5/3}O_4$ system, through NMR, which probes the Li environment, and XAFS, which provides information on both the electronic and structural environment of the Ti. The NMR results have shown that lithium insertion in $Li_{4/3+x}Ti_{5/3}O_4$ is not completely described by a simple conversion from 8a tetrahedral to 16c octahedral lithium sites accompanied by a passive role for $Li_{1/3}Ti_{5/3}O_4$. The NMR data suggest that either the 16c sites are not as abundant as previously thought and/or that new lithium sites are created that coexist along with 8a, 16d and 16c. Line width data show that the homogeneity of lithium ion site distribution is compromised upon cycling. The EXAFS results suggest very little change in structure up to 50% of discharge (or charge), and the onset of a subtle static

disorder (apparently not previously observed by diffraction experiments) occurring at higher x-values. Once this feature sets in, it remains through the fully intercalated material and persists through cycling. The relationship between this apparent (though relatively small) structural irreversibility and the change in Li-site distribution observed by NMR is not yet clear, but both sets of results demonstrate the power of complementary short-range structural probes in revealing subtle features not observed by more conventional means (i.e. X-ray diffraction).

Acknowledgements

This research was supported in part by grants from the Basic Energy Sciences Division of the US Department of Energy and the SCORE Program of the National Institutes of Health.

References

[1] K.M. Colbow, J.R. Dahn, R.R. Haering, J. Power Sources 26 (1989) 397.
[2] T. Ohzuku, A. Ueda, Solid State Ionics 69 (1994) 201.
[3] D.C. Johnston, H. Prakash, W.H. Zachariasen, R. Viswanathan, Mater. Res. Bull. 8 (1973) 777.
[4] T. Ohzuku, A. Ueda, N. Yamamoto, J. Electrochem. Soc. 142 (5) (1995) 1431.
[5] S. Sharner, W. Weppner, P. Schmid-Beurmann, J. Electrochem. Soc. 146 (3) (1999) 857.
[6] S. Panero, P. Reale, F. Ronci, B. Scrosati, P. Perfetti, V. Rossi Albertini, Chem. Phys. 3 (2001) 845.
[7] F. Ronci, P. Reale, B. Scrosati, S. Panero, V. Rossi Albertini, P. Perfetti, M. di Michiel, J. Merino, J. Phys. Chem. B 106 (2002) 3082.
[8] M. Dalton, D.P. Tunstall, J. Todd, S. Arumugam, P.P. Edwards, J. Phys.: Condens. Matter 6 (1994) 8859.
[9] D.P. Tunstall, J.R.M. Todd, S. Arumugam, G. Dai, M. Dalton, P.P. Edwards, Phys. Rev. B 50 (1994) 16541.
[10] J.P. Kartha, D.P. Tunstall, J.T.S. Irvine, J. Solid State Chem. 152 (2000) 397.
[11] Z.Y. Wu, G. Ouvrard, S. Lemaux, P. Moreau, P. Gressier, F. Lemoigno, J. Rouxel, Phys. Rev. Lett. 77 (10) (1996) 2101.
[12] J.E. Gonçalves, S.C. Castro, A.Y. Ramos, M.C.M. Alves, Y. Gushikem, J. Electron. Spectrosc. Relat. Phenom. 114/116 (2001) 307.
[13] F.M. Alamgir, Y. Ito, H. Jain, D.B. Williams, Phil. Mag. Lett. 81 (2001) 213.
[14] E. Fukushima, S.B.W. Roeder, in: Experimental Pulse NMR: a Nuts and Bolts Approach, Addison-Wesley, Reading MA, 1981.
[15] B. Ammundsen, J. Roziere, M. Saiful Islam, J. Phys. Chem. B 101 (1997) 8156.